Electronic structure of metal hydrides. II. Band theory of ScH_2 and YH_2

D. J. Peterman, B. N. Harmon, and J. Marchiando*
Ames Laboratory United States Department of Energy and Department of Physics, Iowa State University, Ames, Iowa 50011

J. H. Weaver
Synchrotron Radiation Center, University of Wisconsin-Madison, Stoughton, Wisconsin 53589
(Received 30 November 1978)

Self-consistent band-structure calculations have been performed for ScH_2 and YH_2 using the Korringa-Kohn-Rostoker method. The results indicate a net charge transfer from the metal to the hydrogen site and a concomitant raising of the hydrogen bonding bands relative to those obtained through non-self-consistent calculations. Comparisons are made between the results of our calculations and the results of optical studies by Weaver, Rosei, and Peterson. Additional calculations were performed in which the Fermi level or band gaps were rigidly shifted by a small energy increment. These calculations were used to simulate the derivative structure obtained in thermomodulation spectra and helped to identify the k-space origin of several experimental interband features found in the thermoreflectance of ScH_2 and YH_2. The experimentally observed, low-energy, stoichiometry-dependent optical features of YH_2, which had partially inspired our studies, were not interpretable within the framework of our calculations based on the CaF_2 structure in which the hydrogen occupies all of the available tetrahedral sites. Instead, indirect evidence suggests that these low-energy features are associated with partial occupation of octahedral sites.

I. INTRODUCTION

Hydrogen in metals is an important and rapidly expanding field of theoretical and experimental study.[1] One of the challenging theoretical areas of study involves the detailed characterization of the electronic structure of metals that contain either a relatively small amount of interstitial dissolved hydrogen (disordered α-phase solutions) or a high density of hydrogen (ordered hydride phases). A theoretical treatment of an "alloy" of a d-band transition metal with hydrogen, the simplest of elements, is, however, fraught with a variety of difficult and intriguing problems. For example, there has been intense discussion regarding the charge character of a single proton moving through or vibrating in a metallic host. Even the question of whether a static proton in a transition metal lattice has a bound state cannot be easily answered.

Treating ordered hydrogen in a monohydride, dihydride, or trihydride is considerably more manageable than treating it when it appears in a disordered hydrogen solution since the ordered hydride can be handled within the framework of band-theoretical methods. The pioneering calculations of Switendick were the first to show the dramatic changes in the band structure of a metal caused by a high density of hydrogen.[2] These calculations demonstrated the complex nature of hydrogen in metals and showed the weaknesses of the numerous simple models which have been proposed to interpret the diverse physical properties of the hydrides (e.g., the protonic and anionic models). Switendick's band model has only recently been supported by the results of photoelectron and optical studies.[3-6] The band model has also been applied to other hydrogen-metal systems. Among these, PdH (PdD) has been the most extensively studied due to its superconducting properties that exhibit an inverse isotope effect.[7] Several recent detailed band calculations[8-10] of PdH have shown that H does not simply give up an electron to the metal bands but rather that there is significant lowering of energy of those states whose wave functions have appreciable amplitude at the interstitial H site and therefore sample the hydrogen potential. It is observed that some formerly empty states are drawn below E_F and that E_F moves upward to just beyond the top of the d bands. For the dihydrides considered in this paper, the effects of hydrogen on the metallic band structure are more dramatic, with additional hydrogenlike states appearing below the Fermi level. However, as we mention in discussing charge transfer, the electronic charge surrounding the hydrogen site is similar in both PdH and the dihydrides.

In the present paper, we approach the general problem of hydrogen in metals by applying the Korringa-Kohn-Rostoker (KKR) band calculational method to study ordered ScH_2 and YH_2. These dihydrides can be viewed as prototypes of the large number of metallic dihydrides which form in the same (or nearly so) CaF_2 fcc structure. Our calculations have been motivated in part by the results of recent optical studies of ScH_2, YH_2, and LuH_2 that revealed many spectral similarities, but also some intriguing differences. When the

preliminary optical experiments with YH_x of varying x (within the single-phase dihydride composition range) proved difficult to interpret from the vantage point of the existing calculations of Switendick, we undertook calculations to examine the importance of self-consistency for determining the electronic structure of YH_2. So that we might better understand the systematics of the trivalent dihydrides, we also considered ScH_2 which has a lattice constant approximately 10% smaller than that of YH_2 and hence a reduced hydrogen-hydrogen separation.

In Sec. II, we give the details and results of our calculations, emphasizing the differences between the self-consistent (SC) and non-self-consistent (NSC) energy bands. We then compare our results with optical-reflectance and thermoreflectance experiments which have been presented in the companion paper[11] (henceforth referred to as I). In Sec. IV, we review pertinent experiments which offer indirect evidence that disorder exists in the hydrogen sublattice of YH_x and the lanthanide dihydrides (LnH_x's) for x approaching 2. The implications that octahedral sites are occupied before all tetrahedral sites are filled are then discussed. We conclude by urging further studies that would examine this disorder and elucidate its effects on the physical properties of these important materials.

II. CALCULATIONAL DETAILS AND RESULTS

Both ScH_2 and YH_2 are reported to have the CaF_2 fcc structure with the metal atoms positioned on an fcc lattice and hydrogen situated at the tetrahedral sites (see Fig. 1 of I). The lattice constants at room temperature for these crystals[12] are given in Table I. The band-structure calculations for these compounds were performed using the standard KKR method which requires the muffin-tin approximation for the crystal potential. The muffin-tin radii were chosen (following Switendick[2]) so that the sphere surrounding the metal site extended 65% of the way to the hydrogen position. Based upon the results of Papaconstantopoulos *et al.*[8] for PdH, we do not expect the d-like energy bands to be particularly sensitive to the relative sphere sizes.

Initial non-self-consistent (NSC) calculations were performed using the full Slater ($\alpha = 1$) approximation for exchange and correlation. The potential was obtained by the usual prescription of overlapping atomic charge densities for the d^2s^1 configuration. All relativistic effects except spin-orbit coupling were included, though these effects are small.[13] The results were in excellent agreement with Switendick's APW results when the KKR wave functions were expanded through $l = 3$ about the metal site and $l = 1$ about the hydrogen site.[2]

Since the full Slater ($\alpha = 1$) approximation has been found to over-estimate the effects of exchange and correlation in SC calculations, we used the Hedin-Lundqvist approximation to obtain the SC bands.[14] This approximation has been successfully used to calculate the SC electronic structure of all the paramagnetic elemental $3d$ and $4d$ transition metals.[15] For each iteration the bands and wave functions were determined at 60 points in the irreducible $\frac{1}{48}$th of the Brillouin zone. The points were chosen using the "special point" formalism of Chadi and Cohen.[16] The core states of the metal were recalculated for each iteration. The eigenenergies and the total charge within the muffin-tin spheres were converged to 0.001 Ry and 0.001 electron, respectively.

The self-consistent band structures for ScH_2 and YH_2 are shown in Figs. 1 and 2. The dotted lines represent the two lowest valence (or bonding) bands from our NSC calculations based on the d^2s^1 atomic configuration and highlight the major differences between our SC and our (or Switendick's) NSC calculations. Those differences are most pronounced in the lower two bands that can best be described as hydrogenlike bonding bands. The wave functions for the Γ_1 state are largely covalent, having a large admixture of both hydrogen s and metal s character. The Γ_2' wave functions are nearly pure

TABLE I. Lattice constants and charge transfers for ScH_2 and YH_2.

Charge inside muffin-tin sphere	ScH_2, $a = 4.783$ Å			YH_2, $a = 5.204$ Å		
	Sc	H	Interstitial	Y	H	Interstitial
Atomic charge	19.019	0.536	•••	36.793	0.578	•••
Overlapping atoms	19.531	0.707	2.055	37.283	0.756	2.205
Charge after final iteration	19.323	0.844	1.989	37.116	0.896	2.093

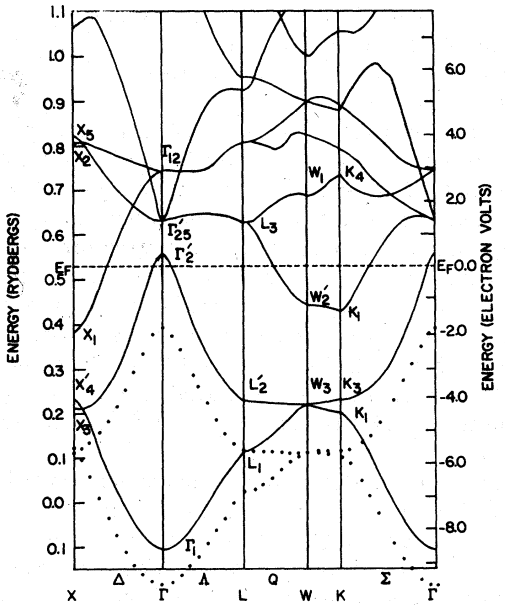

FIG. 1. Self-consistent energy bands of ScH_2 calculated with Hedin-Lundqvist exchange. The lower two bands are *sp-d* hybridized and are termed the bonding bands. The dotted lines indicate the positions of the non-self-consistent ($\alpha = 1$) bonding bands. The bands at E_F (except the pocket around Γ) are *d*-derived and are relatively insensitive to potential approximations. The energy separation of the Γ_{12} and Γ'_{25} states reflects the crystal field splitting of the *d* bands.

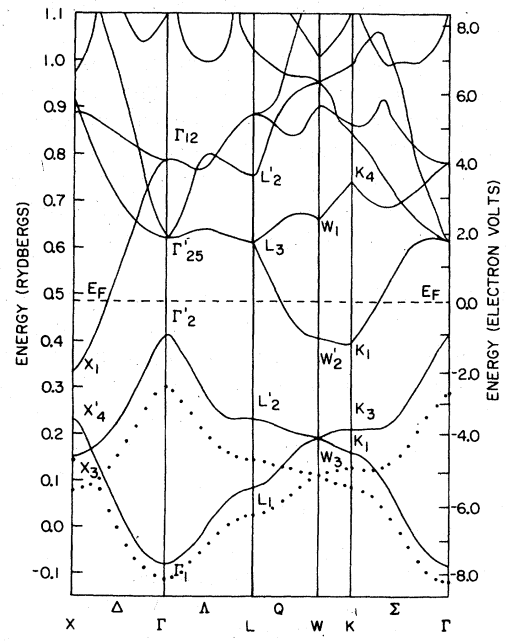

FIG. 2. Self-consistent energy bands of YH_2 (see caption to Fig. 1). For YH_2, the bonding bands are completely below E_F, and the bonding bandwidth, $E(\Gamma'_2) - E(\Gamma_1)$, is approximately 2 eV narrower in YH_2 than in ScH_2.

hydrogen *s*-like (80% of the charge for this state is inside the relatively small hydrogen muffin-tin spheres) and have been described as Bloch sums of antibonding 1*s* orbitals between the two hydrogens in the unit cell[2]; the character of the Γ'_2 wave functions at the metal site is primarily *f*-like. As shown, one effect of Hedin-Lundqvist exchange is to increase the Γ_1 to Γ'_2 separation and thus widen the bonding bands. There is also an overall shift of the two bonding bands upward relative to the metal *d*-like bands. The combination of these two effects causes the Γ'_2 state to rise slightly above the Fermi energy for ScH_2 as shown in Fig. 1. The partially occupied third band and higher bands result from the *d*-derived states of the metal.

The calculated densities of states (DOS) for the first five SC bands of ScH_2 and YH_2 are shown in Figs. 3 and 4, respectively. To obtain the DOS, the calculated first-principles eigenvalues at 84 points were least-squares fit with 45 symmetrized plane waves (the typical rms error was less than 1 mRy). These fits were used to generate the band energies at the corners of 2048 tetrahedra which filled the irreducible $\frac{1}{48}$th of the Brillouin zone. The DOS was then obtained using the linear energy tetrahedron method.[17] The most apparent difference between the DOS of ScH_2 and that of YH_2 is that only one peak derived from the bonding bands is seen in ScH_2 whereas two are seen in YH_2. This difference reflects the character of the flat bands along *L-W-K* and the energies of K_1 and K_3 relative to W_3. Furthermore, ScH_2 has a greater bonding bandwidth than YH_2. This is related to

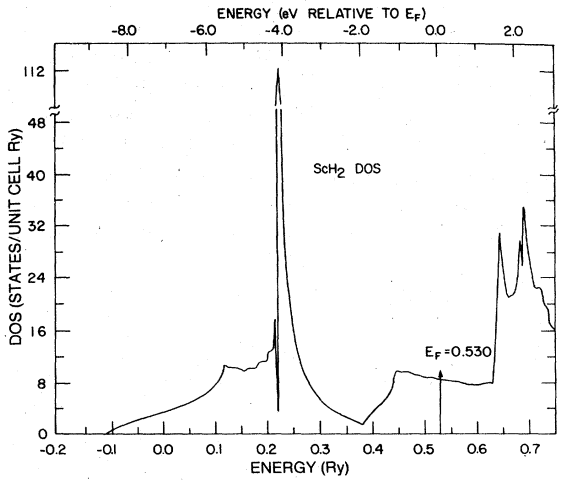

FIG. 3. Electronic density of states (DOS) for the self-consistent energy bands of ScH_2. Only the lowest five bands have been included. The peak at about 4 eV below E_F reflects the position of the flat band extending from L'_2 to K_3 (see Fig. 1.).

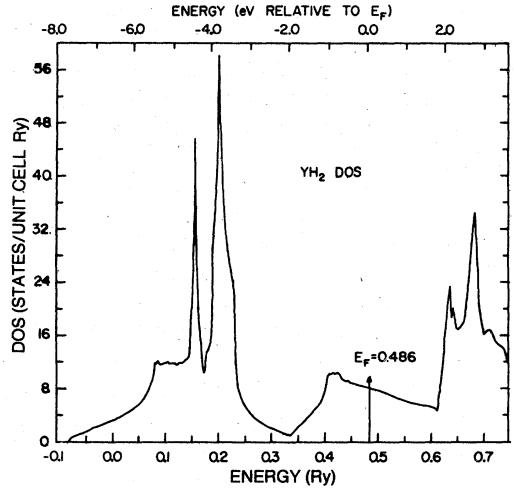

FIG. 4. Electronic density of states (DOS) for the self-consistent energy bands of YH_2. Only the lowest five bands have been included. For YH_2, there is greater dispersion in the bands along L-W-K, and that dispersion is reflected by the double maximum in the DOS ~4 eV below E_F.

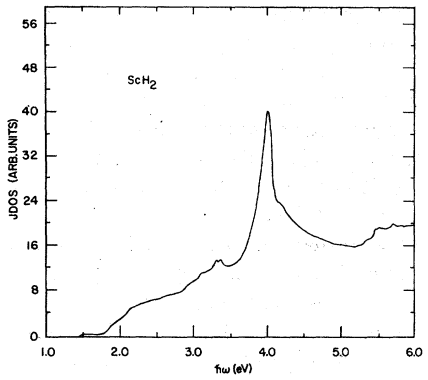

FIG. 5. Joint density of states (JDOS) for the first five bands of (self-consistent) ScH_2. The weak onset at 1.4 eV indicates interband absorption from states near Γ. The stronger onset at 1.7 eV reflects the energy separation of the third and fourth bands along Q.

the smaller lattice spacing in ScH_2, which leads to a larger splitting between the hydrogen bonding (Γ_1) and antibonding (Γ_2') states. Photoemission studies should easily observe these differences.

The joint densities of states (JDOS) for the first five bands are shown in Figs. 5 and 6 for ScH_2 and YH_2, respectively. These were obtained using the techniques already described for the calculation of the DOS. Care was taken to include only the portion of the tetrahedron yielding empty final states or filled initial states whenever the Fermi surface intersected a tetrahedron.

The JDOS is a quantity that, if one neglects the effects of matrix elements for the interband electric dipole transitions, can be used as a guide for assigning optical structures to specific regions of the Brillouin zone. Generally, flat bands at symmetry points or regions of k space where bands are parallel contribute significantly and account for structure in the JDOS. In the JDOS of ScH_2 (Fig. 5), for example, the small feature near 3.3 eV is partly due to transitions between the symmetry points W_1 and W_2' whereas the larger structure near 4.0 eV is largely due to the parallel bands along Σ. The calculated onset of transitions in ScH_2 begins at 1.4 eV and is a result of the Γ_2' state lying close to the Fermi level. The onset of transitions within the ScH_2 d bands occurs at 1.7 eV and the corresponding d-band onset occurs at 2.3 eV in YH_2. The difference in the onset of the d-interband transitions partially reflects the greater width of the d bands of YH_2. This is consistent with the pure metal results which show the d bands in the $3d$ transition metals to be narrower than the d bands of the corresponding $4d$ metals.

The amount and direction of charge transfer is an important quantity in understanding the character of the M-H bond. A precise definition of charge transfer is elusive, however, especially if one wants to specify its magnitude. The results tabulated in Table I define our meaning of charge transfer. The entry labeled "atomic charge" represents the number of electrons of a neutral atom contained within a sphere of radius equal to the muffin-tin radius. If a neutral atom is placed on each appropriate site in the lattice, then the charge inside a muffin-tin sphere is increased above that

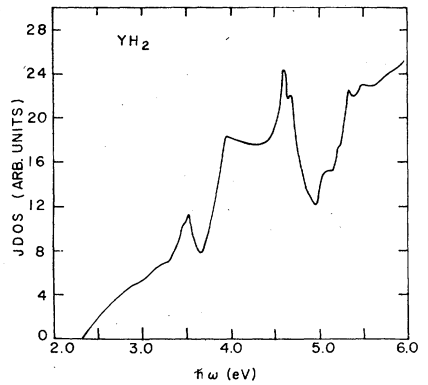

FIG. 6. Joint density of states (JDOS) for the first five bands of (self-consistent) YH_2. The predicted onset for interband absorption occurs at 2.3 eV and is related to transitions from band 3 along Q (at E_F) to band 4. These are observed experimentally as discussed in the text.

of the isolated atom due to the overlapping tails of the neighboring atoms. The entries of Table I indicate that this effect accounts for much of the apparent "screening" of the proton since the charge within the hydrogen muffin-tin sphere is increased by more than 30%. The iterations to self-consistency resulted in a substantial charge transfer (0.14 electron) to the hydrogen sphere, a value quite close to that found for PdH (0.125 electrons).[8] Experimentally, evidence for charge transfer away from Sc sites can be found from x-ray photoemission measurements of the $2p$ core level shifts in ScH_2.[18] In addition, Mössbauer measurements on DyH_2 have given crystal field parameters which indicate a negative charge on the hydrogen sites.[19] This charge transfer toward the hydrogen directly contradicts the protonic or rigid band model which has been too frequently employed for describing metal hydrides.

III. COMPARISON TO OPTICAL EXPERIMENTS

In this section, the optical results of I are discussed in light of our band structure calculations. As we will show, there is good agreement between theory and experiment when we consider the low-x dihydrides. The low-energy features that appear in the experimental spectra for $x \to 2$ cannot be interpreted within the framework of the dihydride calculations, and alternate explanations will be proposed.

If matrix elements are approximately constant throughout the Brillouin zone, one may write

$$\epsilon_2(\omega) \propto |\langle \mathfrak{M} \rangle|^2 \mathcal{J}(\omega)/\omega^2 ,$$

where $\mathfrak{M}$ is a matrix element and $\mathcal{J}(\omega)$ stands for the JDOS. The ϵ_2 spectra of ScH_2 and YH_2 (Fig. 5 of I) can then be compared (when scaled by ω^2) to the calculated JDOS. As can be seen in Figs. 5 and 6, the onset of interband transitions is predicted to occur at 1.4 eV in ScH_2 and 2.3 eV in YH_2. The states that are responsible for the interband onset are different for the two dihydrides because of the different energies of the Γ_2' state (i.e., because the antibonding hydrogen levels are pushed higher in the smaller, more constraining lattice of ScH_2 than in YH_2). For ScH_2, Γ_2' falls above E_F, and the onset of interband absorption, as reflected by the relatively weak feature in the JDOS, is due to transitions from the bonding bands at E_F to final states near the d-like Γ_{25}'. The strong increase in the JDOS of ScH_2 near 1.7 eV and the steep onset in YH_2 at 2.3 eV reflect the large number of states possible for transitions within the d-like complex of bands 3 and 4 along Q, W-K, and Σ.

The experimental onset of interband transitions follows the trend predicted by our calculations: the interband onset (seen in $\epsilon_2\omega^2$) shifts from ~1.25 eV in ScH_2 to ~1.6 eV in YH_2 to ~1.9 eV in LuH_2. These experimental values for the onset energy are from measurements on $ScH_{1.61}$, $YH_{1.73}$, and $LuH_{1.83}$ samples, which are believed to give results representative of the stoichiometric dihydrides with only tetrahedral site occupation.[11] Actual samples of YH_x and LuH_x for $x \simeq 2.0$ show interband transitions beginning at energies as low as 0.2 eV. There is no reasonable way to "adjust" our bands to yield such a low onset for interband transitions. The larger and more systematic onset energies observed for the lower x compounds can, however, be interpreted by making small and plausible changes in the calculated bands.

Although the calculation for ScH_2 predicts the onset of interband absorption to occur at 1.4 eV, we do not expect to observe these transitions. This is because of the extremely small occupied volume associated with the states near Γ_2' (as evidenced in the small magnitude of the JDOS curve of Fig. 4 for energies between 1.4 and 1.7 eV) and the nature of the transition which results in a transfer of charge from the highly localized states about the hydrogen sites to the predominantly d-like states of the metal. We therefore expect the onset of observed transitions to be associated with bands 3 and 4 along Q, W-K, and Σ. The systematic change of the experimental onset energy from ~1.25 eV in ScH_2 to ~1.9 eV in LuH_2 can then be understood as arising from the widening of the d bands which is observed in going from $3d$ to $4d$ to $5d$ transition metals. The theoretical prediction for these onset energies is ~0.4 and ~0.6 eV too large for ScH_2 and YH_2, respectively. This suggests that the calculated d-band separation along Q, W-K, and Σ is too large. This portion of band 3 is somewhat sensitive to the position of the hydrogen bands so that a few tenths of an electron volt discrepancy is not serious. Other aspects of the experimental $\epsilon_2(\omega)$ spectra are not so easily compared with our JDOS calculations since matrix elements have not been included. One optical technique that is less sensitive to the effects of matrix elements is thermomodulation spectroscopy.

Thermomodulation spectroscopy is a valuable way of locating critical points and Fermi surface transitions in the interband absorption of solids. Effects on the physical properties of metals due to a small increase in temperature include: (i) a shifting and/or warping of the energy bands (with a resultant shift of the Fermi level) and a decrease in the plasma frequency due to volume thermal expansion; (ii) a broadening of the step in the Fermi distribution function (thereby chang-

ing the band occupation number for bands at E_F); and (iii) an increase in the phonon population. A small increase in temperature ΔT leads to small temperature-induced changes in the dielectric function, denoted by $\Delta\epsilon_1(\omega)$ and $\Delta\epsilon_2(\omega)$. If matrix element variation with temperature is assumed to be negligible, then we may write

$$\Delta\epsilon_2(\omega) \propto |\langle \mathfrak{M} \rangle|^2 \Delta \mathcal{J}(\omega)/\omega^2 .$$

Thus, structure in $\Delta\epsilon_2(\omega)$ arises from all regions in the Brillouin zone where the temperature dependence of the JDOS is large. These regions are typically located at critical points (usually at symmetry points or along symmetry lines).[20] Other structures can be related to transitions involving bands at E_F since these are highly temperature dependent. The identification of critical points or Fermi surface transitions by their characteristic lineshapes provides considerable information about the electronic structure of the system being studied. The difficult process of lineshape analysis is made easier and more meaningful when supported by band structure calculations.

The derivative structure of $\Delta\epsilon_2$ can be simulated theoretically by considering changes in the joint density of states which result from rigidly shifting a particular band by a small energy increment δ or, in the case of Fermi-level transitions, by shifting the position of the Fermi level. The effect of a shift in the Fermi energy has been examined using the calculated band structure and evaluating

$$\Delta_F \mathcal{J}(\omega) = \tfrac{1}{2}[\mathcal{J}(\omega, E_F + \delta) + \mathcal{J}(\omega, E_F - \delta)] - \mathcal{J}(\omega, E_F) ,$$

where $\delta = 0.01$ Ry. Similarly, the effect of a shift of an energy band (gap shift) has been examined by evaluating

$$\Delta_G \mathcal{J}(\omega) = \tfrac{1}{2}[\mathcal{J}^+(\omega) + \mathcal{J}^-(\omega)] - \mathcal{J}(\omega) ,$$

where $\mathcal{J}^\pm$ are obtained by rigidly shifting a particular band (in our case the fourth band) vertically by ± 5 mRy. These calculated functions will include structure which, due to matrix element effects and broadening, may not be observed experimentally but they are valuable in interpreting experimental data since it can quickly be determined if structure in $\Delta\epsilon_2$ at a certain energy might correspond to a critical point or a Fermi surface transition.

Plots of $\Delta_F \mathcal{J}(\omega)$ for ScH_2 and $\Delta_G \mathcal{J}(\omega)$ for ScH_2 and YH_2 are shown in Figs. 7–9. The first structure in the Fermi-level-shift plot of Fig. 7 for ScH_2 is near 1.4 eV (numbered 1) and is due to transitions around Γ. The most pronounced feature (numbered 2) near 1.7 eV involves the onset within the d-like complex of the third and fourth bands along Q. The structure near 2.7 eV (numbered 3) arises from transitions along Σ and Δ. The Fermi level shift of YH_2 (not shown) displays analogous Fermi surface transitions along Q at 2.3 eV. The energy-gap-shift plots of Figs. 8 and 9 were made by mathematically shifting the fourth bands of ScH_2 and YH_2, respectively. The features at 1.7 eV in the ScH_2 calculation and at 2.3 eV in the YH_2 calculation correspond to the theoretical interband onset between bands 3 and 4 along Q (seen also in the $\Delta_F \mathcal{J}$ calculations). The negative structure at 3.3 eV for ScH_2 (Fig. 8) and at 3.5 eV for YH_2 (Fig. 9) is from transitions between bands 3 and 4 at the symmetry point W. Fourier fitting techniques showed that the bands involved in these transitions, at W_2' and W_1, are responsible for an M_2-type critical point in the JDOS.

The experimental $\Delta\epsilon_1$ and $\Delta\epsilon_2$ spectra for ScH_2, YH_2, and LuH_2 (Fig. 8 of I) display complicated lineshapes below 2–2.5 eV, which include the effects of modulation of the intraband background (monotonically decreasing, structureless, but large at low energy) and the effects of overlapping, modulated interband absorption. The first strong features in $\Delta\epsilon_2$ are due to the modulation of the Fermi-surface transition along Q and probably include the modulation of the Fermi-surface along Σ at ~0.3–0.5 eV higher energy, but it is difficult to identify the characteristic lineshape without ambiguity because of the overlapping contributions from those and higher energy transitions. [From group-theoretical considerations, we find that these Q and Σ (and W) transitions are all electric-dipole-allowed transitions.] A more easily

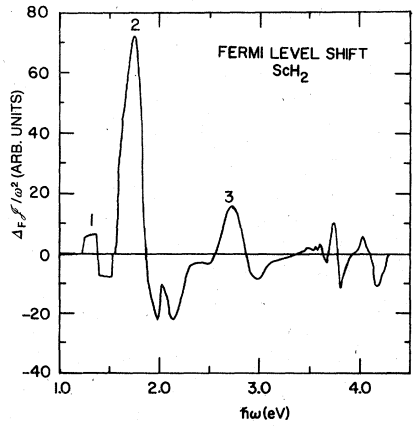

FIG. 7. Calculated change in the JDOS for ScH_2 arising from a mathematical shifting of the Fermi level by 0.01 Ry. Shifting E_F emphasizes predicted JDOS interband transitions which involve states at E_F. Structures labeled by 1–3 can be related to transitions near Γ, along Q, and along Δ and Σ, respectively. Comparisons between theory and experiment are discussed in the text.

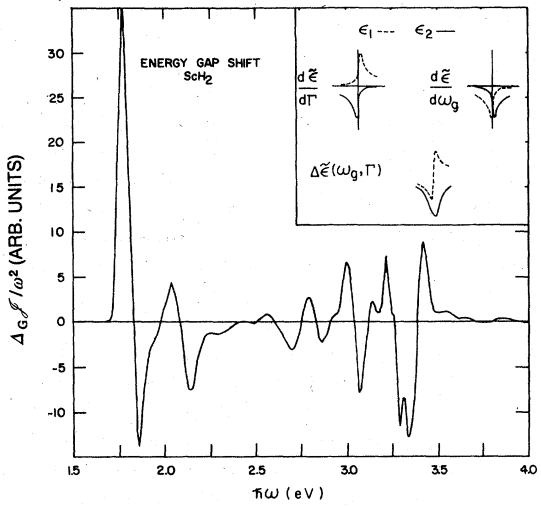

FIG. 8. Calculated change in the JDOS of ScH_2 due to a rigid shift by 5 mRy of the fourth band. The calculated spectra simulate changes in the JDOS due to modulation of the band gap energy and can be compared to thermoreflectance results as is done in the text. The first large derivativelike structure reflects modulation of the transitions along Q at E_F. The feature near 3.3 eV corresponds to the M_2-type critical point transition W_2'-W_1. In the inset, the predicted lineshape for the changes in the dielectric function due to broadening ($d\tilde{\epsilon}/d\Gamma$) and to gap modulation ($d\tilde{\epsilon}/d\omega_g$) of an M_2 critical point transition are shown. These are also compared with experiment in the text.

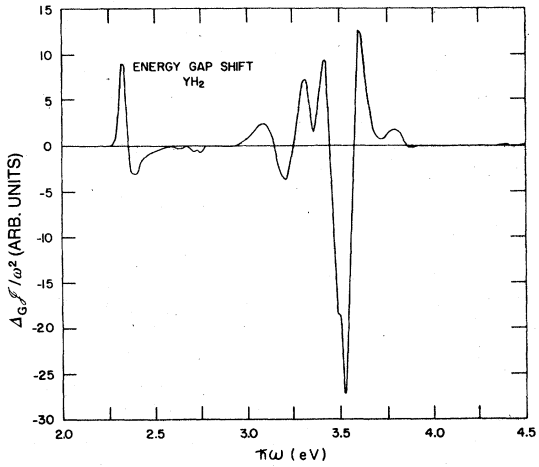

FIG. 9. Calculated change in the JDOS of YH_2 due to a rigid shift by 5 mRy of the fourth band. See caption of Fig. 8.

identifiable lineshape occurs in the experimental spectra at ~2.95 eV in ScH_2, at ~3.1 eV in YH_2, and ~3.15 eV in LuH_2. The minimum in $\Delta\epsilon_2$ at the same energy as a positive-going anti-symmetric structure in $\Delta\epsilon_1$ is characteristic of an M_2-type critical point where lifetime broadening and band gap shifts are the major effects of the modulation (see the inset of Fig. 8). Hence, we suggest that the experimental feature near 2.95 in ScH_2 and 3.1 eV in YH_2 reflect interband transitions at W, namely, the $W_2' - W_1$ transitions that are theoretically predicted at 3.3 and 3.5 eV. Again, there is quite-reasonable agreement between theory and experiment and again the experiment seems to indicate that the calculated separation of the d-bands along Q, W-K, and Σ is somewhat larger than it should be. We do not consider this discrepancy to be too severe, bearing in mind the historical difficulties of adequately treating the itinerant d's in elemental transition metals.

IV. DISCUSSION

Although we have demonstrated reasonable agreement between theory and experimental $\tilde{\epsilon}$ and $\Delta\tilde{\epsilon}$ spectra, the interband transitions giving rise to the low energy features in $YH_x, x \to 2$ (Figs. 3 and 4 of I) cannot be explained using the calculated bands. Any adjustment of the bands to account for interband transitions observed at ~0.4 and 1.1 eV in $YH_{1.96}$ would be aphysical and would destroy the agreement we do have with experimental d-band features. The insensitivity of the d-like bands to both the effects of potential approximation and self-consistency as well as the observed x dependence of the low-energy features in YH_x and the lanthanide dihydrides lead us to the suspicion that a sample-related phenomena, such as the "premature" occupation of octahedral sites, is responsible for the low energy optical absorption. Hence, we postulate a gradual filling of octahedral sites (i.e., some deviation from the purely tetrahedral dihydride pictured in Fig. 1 of I), which occurs before all of the tetrahedral sites are filled. The broadening of the d band features, as discussed in I, could then be understood as arising from lattice disorder caused by the octahedral site occupation—disorder which increases as $x \to 2$ rather than decreases as would be expected for disorder related to tetrahedral vacancies for substoichiometric systems.

Although a calculation involving approximately 20% octahedral site occupation and 90% tetrahedral site occupation is beyond the scope of this paper, it seems reasonable to assume that such a calculation would show some states lowered to near E_F. Such a lowering of empty states to or below E_F has been predicted in the trihydride calculation by Switendick and supported by the photoemission studies of ThH_2 and Th_4H_{15} by Weaver *et al.*[3] Interband transitions involving those states could

account for the low-energy optical structure.

There is considerable indirect evidence, in addition to the concentration and preparation dependence presented in I, that octahedral sites may indeed be occupied. Scandium does not form a trihydride and no more than 2 hydrogen atoms per Sc atom can occupy the fcc structure. Yttrium not only forms a trihydride (with a hexagonal metal lattice), but the fcc lattice accommodates more than 2 hydrogen atoms per Y atom.[21] It is, therefore, plausible that octahederal site occupation is taking place in the yttrium dihydride samples and one reason for this different behavior could be the smaller lattice constant of the Sc compound. LaH_2 has a lattice constant larger than that of YH_2 and also exhibits the low energy interband transition as stoichiometry is approached.[22] In fact, based on their NMR studies, Schreiber and Cotts[23] suggested that the strongly concentration-dependent line narrowing in LaH_x for $x>1.92$ was due to filling of octahedral sites. They believed, however, that this filling of octahedral sites was caused by large numbers of the tetrahedral sites being, for some reason, unavailable, whereas we believe the octahedral occupation is an intrinsic property. It seems once one obtains a large tetrahedral occupation for some dihydride systems, the octahedral sites become energetically more favorable for hydrogen occupation.

Further indirect support for octahedral occupancy can be found in recent Mössbauer measurements[19] of DyH_2. Also, inelastic neutron scattering on $CeH_{1.98}$ yielded a small, isolated peak attributed to localized vibrations of hydrogen occupying a few percent of the octahedral sites.[24] Interestingly, other neutron diffraction measurements on $CeD_{2.0}$ reported a perfect CaF_2 structure,[25] so that questions of isotope effects and sample preparation arise.

The arguments presented for hydrogen occupation of octahedral sites in YH_2 point to areas where more experimental and theoretical investigations are needed. Optical measurements that appear to be measuring the effects of small amounts of octahedral hydrogen are a highly effective way of studying disorder in these compounds. Neutron diffraction and/or NMR studies of the same samples studied by optical measurements might help clarify the degree of disorder. Since these new states which give rise to the low-energy optical transitions must be near the Fermi level, resistivity, heat capacity, and other Fermi-surface-sensitive experiments should also add to the understanding of this phenomenon. If these methods prove to be valuable tools in the investigation of stoichiometry, much could be added to the advancement of preparation techniques and to the characterization of the intrinsic properties of the dihydrides. Theoretical studies of the effects of disorder would also be useful, perhaps along the lines of the CPA calculation of Faulkner[8] for PdH_x using band structures for cubic YH_2 and YH_3. Supercell calculations are also a potentially useful approach for studying the electronic structure of the non-stoichiometric systems. Given enough experimental data and supportive theoretical efforts, a better understanding should evolve.

ACKNOWLEDGMENTS

The authors wish to express their appreciation to D. W. Lynch, S. H. Liu, and D. T. Peterson for their many helpful discussions and continuing encouragement. They also wish to thank G. K. Shenoy and B. D. Dunlap for sending a preprint of Ref. 19. The authors profited from stimulating discussions with A. C. Switendick, R. G. Barnes, D. Torgeson, K. A. Gschneidner, Jr., and others. This work was supported by the U. S. Department of Energy, Office of Basic Energy Sciences, Materials Sciences Division, and the NSF (Grant No. DMR 7721888).

---

*Present address, Natl. Bur. Stand., Building 220, Room A123, Wash., D. C. 20234.

[1]See, for example, D. G. Westlake, C. B. Satterthwaite, and J. H. Weaver, Phys. Today, Nov. 1978, p. 32.

[2]A. C. Switendick, Ber. Bunsenges Phys. Chem. 76, 535 (1972); Solid State Commun. 8, 1463 (1970); J. Less-Common Met. 49, 283 (1976); Int. J. Quant. Chem. 5, 459 (1971).

[3]J. H. Weaver, J. A. Knapp, D. E. Eastman, D. T. Peterson, and C. B. Satterthwaite, Phys. Rev. Lett. 39, 639 (1977).

[4]D. E. Eastman, J. K. Cashion, and A. C. Switendick, Phys. Rev. Lett. 27, 35 (1971).

[5]J. H. Weaver, R. Rosei, and D. T. Peterson, Solid State Commun. 25, 201 (1978); J. H. Weaver and D. T. Peterson, Phys. Lett. A 62, 433 (1977).

[6]J. H. Weaver, Bull. Am. Phys. Soc. 23, 295 (1978).

[7]C. B. Satterthwaite and J. L. Toepke, Phys. Rev. Lett. 25, 741 (1970); T. Skoskiewicz, Phys. Status Solidi A 11, K123 (1972); B. Stritzker and W. Buckel, Z. Phys. 257, 1 (1972).

[8]D. A. Papaconstantopoulos, B. M. Klein, E. C. Economou, and L. L. Boyer, Phys. Rev. B 17, 141 (1978); J. S. Faulkner, *ibid.* 13, 2391 (1976).

[9]C. D. Gelatt, H. Ehrenreich, and J. A. Weiss, Phys. Rev. B 17, 1940 (1978).

[10]M. Gupta and A. J. Freeman, Phys. Rev. B 17, 3029 (1978). M. Gupta has communicated the results of unpublished calculations of TiH_2, TbH_2, and ErH_2.

[11]J. H. Weaver, R. Rosei, and D. T. Peterson, pre-

ceding paper, Phys. Rev. B 19, 4855 (1979).
[12]W. M. Mueller, J. P. Blackledge, and G. G. Libowitz, *Metal Hydrides* (Academic, New York, 1968).
[13]D. D. Koelling and B. N. Harmon, J. Phys. C 10, 3107 (1977).
[14]L. Hedin and B. I. Lundqvist, J. Phys. C 4, 2064 (1971).
[15]V. L. Moruzzi, A. R. Williams, and J. F. Janak, Phys. Rev. B 15, 2854 (1977).
[16]D. J. Chadi and M. L. Cohen, Phys. Rev. B 8, 5747 (1973).
[17]O. Jepsen and O. K. Andersen, Solid State Commun. 9, 1763 (1971); G. Lehmann and M. Taut, Phys. Status Solidi B 54, 469 (1972).
[18]J. K. Gimzewski, D. J. Fabian, L. M. Watson, and S. Affrossman, J. Phys. F 7, L305 (1977).
[19]J. M. Freidt, G. K. Shenoy, B. D. Dunlap, D. J. Westlake, and A. T. Aldred, Phys. Rev. B (to be published).
[20]For a discussion of thermomodulation spectroscopy and critical points, see, for example, B. Batz, in *Semiconductors and Semimetals*, Vol. 9, edited by R. Willardson and A. Beer (Academic, New York, 1972), Chapter 4.
[21]A. Pebler and W. E. Wallace, J. Phys. Chem. 66, 148 (1962).
[22]J. H. Weaver and D. T. Peterson, unpublished data on several LnH_x's.
[23]D. S. Schreiber and R. M. Cotts, Phys. Rev. 131, 1118 (1963).
[24]P. Vorderwisch and S. Hautecler, Phys. Status Solidi B 66, 595 (1974).
[25]A. K. Cheetham and B. E. F. Fender, J. Phys. C 5, L35 (1972).